ESC European Heart Journal - Imaging Methods and Practice (2026) 4, qyag100
https://doi.org/10.1093/ehjimp/qyag100

ORIGINAL ARTICLE
Cardiac magnetic resonance

High resolution, 3D isotropic late gadolinium enhanced imaging for the quantification of left atrial fibrosis and post-ablation scarring

Maximilian Fenski [1,2,3,4,*†], Richard Hickstein [1,2,5,6,†], Leo Dyke Krüger [1,2], Clemens Ammann [1,2,3,5], Thomas Hadler [1,2,5], Karl Kunze [7], Michaela Schmidt[8], René M. Botnar[9,10,11], Claudia Prieto[9,10,11], André Rudolph[3], Marcel Prothmann[3], Michael Wiedemann[3], Thomas H. Grandy [3], and Jeanette Schulz-Menger [1,2,3,5]

[1]Experimental and Clinical Resarch Center, Charité—Universitätsmedizin Berlin, Corporate Member of Freie Universität Berlin and Humboldt Universität zu Berlin, Lindenberger Weg 80, 13125 Berlin, Germany
[2]Working Group on Cardiovascular Magnetic Resonance, Experimental and Clinical Research Center, A Cooperation Between Charité—Universitätsmedizin Berlin and the Max Delbrück Center for Molecular Medicine in the Helmholtz Association, Lindenberger Weg 80, Berlin 13125, Germany
[3]Department for Cardiology and Nephrology, HELIOS Hospital Berlin-Buch, Schwanebecker Chaussee 50, 13125 Berlin, Germany
[4]Radcliffe Department of Medicine, Division of Cardiovascular Medicine, University of Oxford, John Radcliffe Hospital, Headington, Oxford OX3 9DU, UK
[5]DZHK (German Centre for Cardiovascular Research), partner Site Berlin, Berlin, Germany
[6]Faculty IV Electrical engineering and computer science, Technische Universität Berlin, Berlin, Germany
[7]Research & Clinical Translation, Magnetic Resonance, Siemens Healthcare Limited, Camberley, UK
[8]Research & Clinical Translation, Magnetic Resonance, Siemens Healthineers AG, Erlangen, Germany
[9]School of Biomedical Engineering, King´s College London, London, UK
[10]School of Engineering and Institute for Biological and Medical Engineering, Santiago, Chile
[11]Millennium Institute iHEALTH, Santiago, Chile

Received 8 February 2026; accepted after revision 21 May 2026; online publish-ahead-of-print 12 June 2026

Abstract

Aims

Left atrial (LA) myopathy is a key driver of atrial fibrillation (AF) development and progression. Late gadolinium enhancement (LGE) cardiovascular magnetic resonance enables non-invasive quantification of LA fibrosis, a hallmark of atrial myopathy. However, conventional LGE sequences lack sufficient spatial resolution to accurately depict the thin atrial wall, and reference data in healthy cohorts are scarce. This study aimed to evaluate a high-resolution isotropic 3D LGE Dixon sequence for assessing LA fibrosis in healthy controls and AF patients.

Methods and results

In this prospective study, 40 ablation-naïve AF patients (21 paroxysmal, 19 persistent) and 20 healthy controls underwent isotropic (1.3 mm^3) 3D whole-heart LGE imaging. Segmentation was successfully performed using CemrgApp in all participants. A setup-specific threshold for fibrosis detection was defined as an image-intensity ratio (IIR) > 1.34 (mean + 2SD of healthy controls) and validated against pre-procedural electroanatomical mapping (EAM) and follow-up imaging at six months post ablation. At baseline, total LA enhancement was higher in persistent than paroxysmal AF (3.65% [1.84–7.16] vs. 1.16% [0.43–2.27]; $P = 0.044$) and controls (1.25% [0.65–1.75]; $P = 0.041$). No significant correlation was observed between total LGE-derived fibrosis and bipolar low-voltage area ($\rho = -0.03$, $P = 0.87$), though point-by-point analysis showed a weak negative correlation ($\rho = -0.05$, $P < 0.001$). In patients with sinus rhythm at follow-up, total fibrosis increased from 1.68%

* Corresponding author. E-mail: maximilian.fenski@charite.de
† Both authors contributed equally.
© The Author(s) 2026. Published by Oxford University Press on behalf of the European Society of Cardiology.
This is an Open Access article distributed under the terms of the Creative Commons Attribution-NonCommercial License (https://creativecommons.org/licenses/by-nc/4.0/), which permits non-commercial re-use, distribution, and reproduction in any medium, provided the original work is properly cited. For commercial re-use, please contact reprints@oup.com for reprints and translation rights for reprints. All other permissions can be obtained through our RightsLink service via the Permissions link on the article page on our site—for further information please contact journals.permissions@oup.com.

[0.64–6.51] to 6.30% [2.53–12.28]; $P < 0.001$, driven by peri-ablational scar formation, with no change in remote myocardium. Intra-reader correlation for LA-LGE was excellent: ICC 0.99 (95% CI 0.95–0.99).

Conclusion High resolution isotropic 3D LA-LGE enables robust detection of ablation-induced scarring and biologically plausible fibrosis differences between AF stages. However, its correlation with bipolar voltage mapping remains limited, suggesting that LGE and EAM provide complementary information on atrial myopathy.

Graphical Abstract

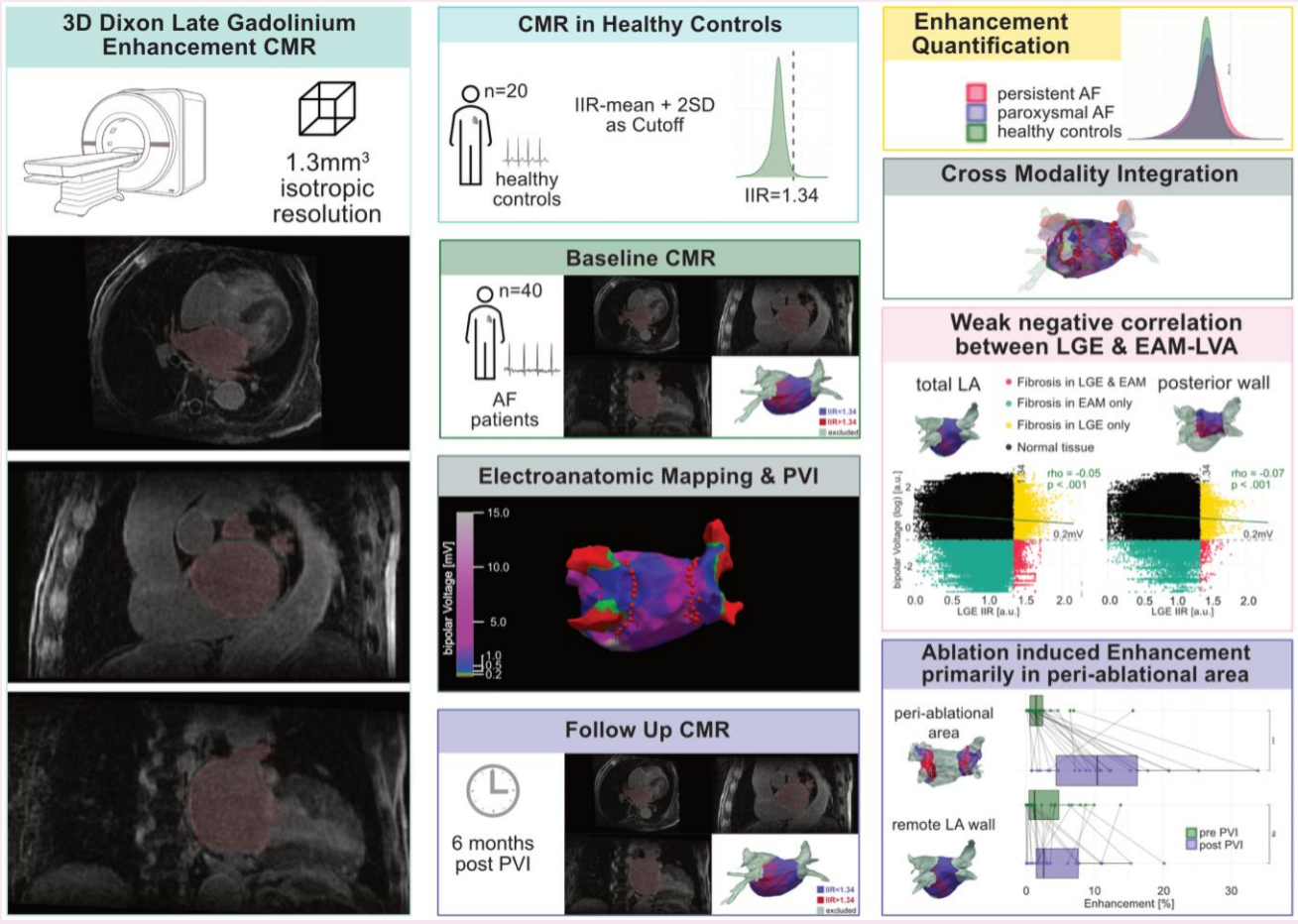

Keywords atrial fibrillation • left atrial fibrosis • late gadolinium enhancement • electroanatomical mapping • cardiovascular magnetic resonance • left atrial myopathy

Introduction

Left atrial (LA) myopathy has been recognized to promote the development and progression of atrial fibrillation (AF).[1] Fibrosis deposition is a hallmark of atrial myopathy, increases with AF progression and carries prognostic relevance.[2,3] While histopathology remains the gold standard for assessing atrial fibrosis,[4] routine application in patients is not feasible. Electroanatomical mapping (EAM)–derived bipolar low-voltage areas are accepted surrogates for atrial fibrosis but require invasive procedures.[5]

Late gadolinium enhancement (LGE) cardiovascular magnetic resonance (CMR) has emerged as a non-invasive alternative for evaluating LA fibrosis, with potential applications in risk stratification,[6] ablation guidance,[7,8] prediction of treatment success,[9] and assessment of ablation lesions.[10] Some studies reported predictive value for AF recurrence[9] and correlations between LGE signal intensity and atrial voltage[11,12]; however, these findings have not been consistently reproduced, even with high-density EAM and comparable post-processing approaches.[13–15]

The limited reproducibility likely reflects technical challenges. The spatial resolution of conventional LA-LGE exceeds atrial

wall thickness in at least one dimension,[16] and anisotropic voxel sizing introduces measurement inaccuracies.[17] Moreover, accurate identification of pathological changes requires a clear understanding of the normal LA appearance; however, data describing LGE signal characteristics in healthy atria remain scarce.

Recent advances in 3D LGE imaging now permit isotropic, high-resolution acquisitions (1.3 mm^3), potentially enabling a more accurate depiction of LA fibrosis.[18] This technique, however, has not yet been validated for the assessment of LA fibrosis.

The aim of this study was to evaluate high-resolution 3D LGE for the assessment of LA fibrosis and ablation induced scarring. Specifically, we sought to (1) establish a setup-specific normality threshold using healthy controls, (2) examine the correlation between LGE-derived fibrosis and high-density EAM voltage, and (3) assess the ability of high resolution LGE to detect ablation-induced scar at follow-up.

Methods

Study design and population

This prospective study included ablation-naïve patients with symptomatic AF before undergoing catheter ablation for pulmonary vein isolation (PVI) at one tertiary care centre. Healthy subjects were included to form a control group. All AF patients underwent baseline CMR on the day of or one day before the ablation procedure. Participants presenting with AF were cardioverted into sinus rhythm to avoid arrythmia-induced motion artefacts. AF patients who could not remain in sinus rhythm or with incomplete isolation of all pulmonary veins were excluded from the study. Further exclusion criteria included contraindications to CMR or gadolinium-based contrast media, and claustrophobia. AF status (i.e. paroxysmal or persistent) was classified using ESC guideline criteria.[19] All AF patients were scheduled for 96-hour Holter monitoring and follow-up CMR at six months post-ablation. Arrhythmia recurrence was defined as any documented episode of AF, atypical atrial flutter or atrial tachycardia lasting >30 s after a three-month blanking period. Healthy controls were referred for CMR to assess for a potential cardiac disease but had (1) no structural or functional abnormalities on CMR, (2) normal sinus rhythm on resting ECG, (3) no history of cardiovascular disease and (4) did not take any systemic medication. All subjects provided written informed consent to participate. Ethical approval was granted by the institutional ethics committee under EA1/111/18.

CMR protocol

Images were obtained using a 1.5T scanner (AvantoFit, Siemens Healtineers, Forchheim, Germany), ECG gating and a 32-channel surface phased-array coil. For the assessment of cardiac function and volumes, cine images with 30 phases were acquired in four long-axis views, consisting of a four-, two-, and three-chamber view, as well as a right ventricular view, and one short-axis stack covering both ventricles. Baseline and follow-up imaging followed the same protocol.

LA-LGE imaging

To assess LA fibrosis, an image-navigated free-breathing whole heart 3D fat/water-separated LGE research sequence[18] with isotropic spatial resolution (1.3 mm^3) was acquired in transversal orientation ~15 min after application of 0.2 mmol/kg Gadoteridol. Typical sequence parameters were: FOV 320 mm × 320 mm × 104 mm, TR: 7.2 ms, TE1: 2.38 ms; TE2: 4.76 ms; FA: 20°. The inversion time (TI) was determined per patient using a TI-Scout. To account for the time delay between TI scouting and image acquisition, 21 ms were added on average. Data was acquired during the most quiescent phase of the heart which was determined using 4CV cine imaging.

Image analysis

LGE-derived fibrosis estimation was performed using open source software CemrgApp (v2018.4.02)[20] and the previously described image-intensity ratio (IIR) approach. This approach normalizes LGE intensities to the blood pool to account for inter scan variability.[11] Segmentation of the LA was conducted directly on fat-suppressed axial 3D LGE images by manually contouring the LA epicardium to create an atrial surface shell. For each LA surface cell, the maximum signal intensity along its corresponding normal (length: 3 voxel inwards, 1 voxel outwards) was projected onto the surface of the LA shell and normalized against the mean blood pool signal intensity. Mean blood pool intensity was identified automatically, based on the mean voxel intensity inside the LA segmentation with a minimum distance of 3 voxels from the LA wall. The pulmonary veins, mitral valve and left atrial appendage were manually excluded before further analysis. An IIR threshold to distinguish between healthy and fibrotic LA wall was defined as the healthy control group's mean IIR plus two standard deviations (SD).[21] Assessment of the distribution of IIR values and testing for the best-fitting distribution model are provided in the Supplementary Material. Once the threshold had been determined, the percentage of LA enhancement was calculated as the number of cells in the LA wall shell with values above the threshold divided by the total number of cells. To assess intrareader variability, a blinded repeated LA-LGE image analysis was performed for ten cases, with at least three months between reads. Assessment of atrial and ventricular function and dimensions was performed according to recent guidelines.[22]

Electro-anatomical mapping and ablation procedure

Bipolar endocardial LA voltage maps were acquired in sinus rhythm prior to catheter ablation using either a 20-polar Lasso-Nav or a Pentaray mapping catheter in combination with CARTO-3 (*Biosense Webster, Diamond Bar, CA)*. Efforts were made to distribute measurement points evenly throughout the LA. Detailed mapping settings can be found in the supplement. Following the mapping procedure, circumferential PVI was achieved using an irrigated-tip, contact force-enabled radiofrequency ablation catheter (Thermocool Smart Touch, tip electrode: 3.5 mm, interelectrode spacing: 2–5–2 mm, Biosense Webster, CA). Radiofrequency energy of up to 35 W was applied at each point for 30–60 s. Additional linear lesions were not performed. Complete PVI was defined as bi-directional conduction block.

Image and electroanatomical mapping registration

The reconstructed 3D EAM LA geometry was transferred from CARTO-3 into open-source software Paraview (version 5.10.0) and the pulmonary veins, left atrial appendage and the mitral valve were manually excluded before further analyses. Prior to quantitative analyses, excluded areas on LA-LGE and CARTO maps were inspected to ensure minimal discrepancies between excluded areas in both modalities. The relative fibrotic surface amount was calculated as the number of surface cells with a bipolar voltage < 0.5 mV divided by the total number of surface cells. To allow point-to-point and regional correlation between LGE and EAM, we used rigid and non-rigid registration to align the two 3D volumes using custom software (for a detailed description see supplementary material). The posterior wall was defined based on a recent consensus.[23] To assess ablation induced changes in the peri-ablational and remote LA myocardium, baseline and follow-up LGE surface models were co-registered to the EAM geometry. Ablation points were projected onto the LA-LGE shells. The peri-ablational area was defined as the LA myocardium within ±7.5 mm surface distance from ablation sites.[24] For an overview of the analysis pipeline refer to *Figure 1*.

Statistical analysis

Continuous variables are presented as mean ± SD or median [interquartile range], depending on their distribution. Categorical

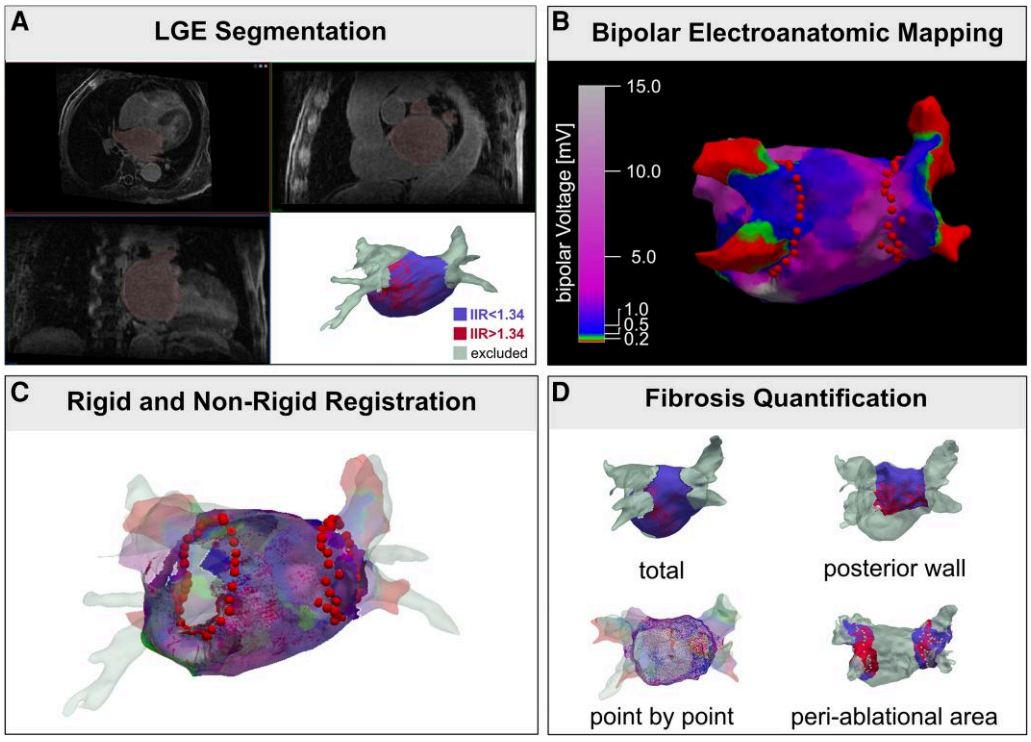

Figure 1 (*A*) The left atrium (LA) was manually segmented on late gadolinium enhanced (LGE) images, and blood pool normalized image intensities (IIR) were projected onto a 3D surface model. Pulmonary veins and the mitral valve were excluded from analysis (excluded areas shown in grey). Fibrosis (defined as IIR values >1.34 based on a healthy control group's mean plus 2 standard deviations) is shown in red, non-fibrotic tissue (IIR <1.34) in purple. (*B*) Bipolar electroanatomic mapping (EAM) was performed prior to pulmonary vein isolation (red dots indicate ablation sites). (*C*) EAM and LGE datasets were co-registered using rigid and non-rigid surface registration. (*D*) Quantification of LA fibrosis was performed 1) for the total LA surface 2) regional for the posterior wall only 3) on a point-by-point basis and 4) within peri-ablational regions in comparison to the remote myocardium.

variables are presented as frequencies and percentages and compared using χ^2 analysis or Fisher's exact test. Differences between groups were evaluated with *t*- or Mann-Whitney-U tests (two groups) and with ANOVA or Kruskal-Wallis tests (three groups) as appropriate. Post-hoc testing was performed using Tukey's range test or Dunn's test respectively. Differences between baseline and follow-up measurements were assessed using paired *t*- or Wilcoxon Signed-Rank Test. Relations between LGE and EAM data was evaluated using Spearman's rank correlation. Intraclass correlation coefficient (ICC) and Bland-Altman analysis was used to assess intrareader reliability. A probability value <0.05 was considered statistically significant. The statistical analyses were performed in R 4.3.2 using the core library's stats package and the FSA (0.10.0) package (Dunn's-Test). Interreader analysis was conducted in Matlab R2023b.

Results

Cohort

Our cohort included 40 ablation-naïve patients with AF. In this cohort, 21/40 (53%) had paroxysmal and 19/40 (47%) had persistent AF. The median age was 70 (62–74) years and 26/40 (65%) were male. A total of 14 (74%) patients with persistent AF presented in AF and were cardioverted into sinus rhythm before undergoing CMR. One patient with paroxysmal AF presented in AF but converted spontaneously into sinus rhythm. AF was recently diagnosed in most included patients with median disease duration of 126 (65–365) days. Disease duration, CHA_2DS_2-Vasc scores and assigned medical treatment did not differ between the two patient groups ($P > 0.05$ for all). Healthy controls ($n = 20$) included eight men (40%) and the median age was 39 years (34–43). Two volunteers were excluded after LGE imaging showed focal high signal intensities in the LA wall. The baseline demographic and clinical characteristics can be found in *Table 1*. *Table 2* shows measurements of left ventricular and atrial size and function.

LGE results

Based on the healthy control group's mean IIR + 2SD, a threshold of 1.34 was obtained. This threshold was applied to all further analysis. See *Figure 2* for the groups' IIR distributions.

Differences between groups

Persistent AF patients showed higher amounts of total LA enhancement (3.65% [1.84–7.16]) compared with paroxysmal AF patients (1.16% [0.43–2.27], $P = 0.044$) and healthy controls (1.25% [0.65–1.75], $P = 0.041$). (*Figure 3*). There was no significant difference between paroxysmal AF and healthy controls ($P = 1.00$).

Table 1 Baseline characteristics

	Control (*n* = 20)	Px-AF (*N* = 21)	Ps-AF (*N* = 19)	*P*
Age, years	36.0 (33.3–43.0)	71.0 (25.4–76.0)[a]	69.0 (62.0–71.0)[a]	<0.001
Male, *n* (%)	9 (45)	8 (38)	18 (95)[a,b]	<0.001
BMI, kg/m^2	24.1 (22.4–26.0)	28.4 (25.4–31.0)[a]	29.4 (25.2–33.1)[a]	0.001
Sinus rhythm at baseline, *n* (%)	20 (100)	20 (95)	5 (26)[a,b]	<0.001
Heart rate, bpm	74 ± 15	61 ± 9.4[a]	71.9 ± 11.5[b]	0.005
CHA2DS2-Vasc Score	N/A	3 (2–4)	2 (1–3)	0.069
Median days since AF diagnosis (IQR)	N/A	87 (61–198)	168 (97–613)	0.161
Diabetes, *n* (%)	0 (0)	6 (29)	2 (11)	0.241
Hypertension, *n* (%)		15 (75)	14 (74)	0.873
Hyperlipidemia, *n* (%)	0 (0)	10 (48)	6 32)	0.301
Heart failure, *n* (%)	0 (0)	2 (10)	2 11)	0.916
CAD, *n* (%)	0 (0)	5 (24)	3 (16)	0.698
Stroke, TIA or arterial thromboembolism, *n* (%)	0 (0)	3 (14)	3 (16)	0.916
Peripheral vascular disease, *n* (%)	0 (0)	4 (19)	4 (21)	0.874

Values are shown as mean ± SD, median (IQR) or *N* (%).
Px-AF, patients with paroxysmal AF; Ps-AF, patients with persistent AF.
[a]*P* < 0.05 vs. Healthy Controls.
[b]*P* < 0.05 vs. Px-AF.

Table 2 Left ventricular and atrial size and function at baseline

	Control (*n* = 20)	Px-AF (*N* = 21)	Ps-AF (*N* = 19)	*P*
Left ventricle				
LV EDV-I, mL/m^2	87.4 ± 16.4	82.3 ± 17.9	86.8 ± 19.1	0.612
LVEF, %	60.1 ± 4.1	59.7 ± 7.7	56.6 ± 7.3	0.221
LV Mass-I, g/m^2	35.8 ± 9.9	45.4 ± 10.8[a]	49.6 ± 11.2[a]	<0.001
Left atrium				
LAV-I mL/m^2	38.0 ± 12.0	45.1 ± 9.4[a]	59.3 ± 18.0[a,b]	<0.001
LAEF, %	68.8 ± 6.6	51.1 ± 11.7[a]	36.2 ± 14.1[a,b]	<0.001
LA LGE, %	1.25% [0.65–1.75]	1.16 [0.43–2.27]	3.65 [1.84–7.16][a,b]	0.018

Values are shown as mean ± SD or median (IQR).
Px-AF, patients with paroxysmal AF; Ps-AF, patients with persistent AF.
[a]*P* < 0.05 vs. Healthy Controls.
[b]*P* < 0.05 vs. Px-AF.

Correlation with disease duration

A weak and nonsignificant correlation (spearman) rho = 0.27, *P* = 0.154 was observed between self-reported disease duration and total LGE-scar burden in AF patients.

Relation between LGE and EAM

Thirty patients had EAM data available. In ten patients, high-density mapping in CARTO was not performed due to logistical reasons. A mean of 1032 ± 562 mapping sites per patient was acquired. The total fibrotic burden assessed by EAM was higher (18.93% [8.12–26.34]) than that assessed by LGE (1.53% [0.49–6.26], *P* < 0.001). In the posterior wall, fibrotic burden was higher for LGE (1.28% [0.17–3.35] compared with EAM (0.11% [0.00–1.29], *P* = 0.030). On a per patient level, no correlation was observed between fibrotic burden assessed by LGE and EAM for the total atrial surface (rho = –0.03, *P* = 0.869) or the posterior wall (rho = 0.14, *P* = 0.484) (*Figure 4*). Point-by-point analysis revealed a very weak but significant negative correlation between IIR and bipolar voltage for both the total LA surface (rho = –0.05, *P* < 0.001) and the posterior wall (rho = –0.07, *P* < 0.001) (*Figure 5*).

Follow-up imaging: assessment of scar formation

At six-month follow-up, LA-LGE was available in 29 patients without recurrence. *Figure 6* shows the study flow-chart. The total fibrotic burden increased from baseline (1.68% [0.64–6.51]) to follow-up (6.3% [2.53–12.28], *P* < 0.001). Regional analysis attributed this increase to peri-ablational scar formation with an absolute increase of 8.58% [2.05–13.60], *P* < 0.001 from

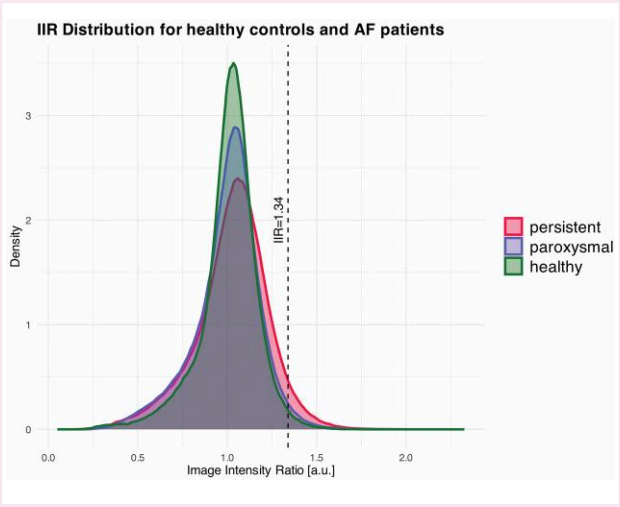

Figure 2 Image intensity ratio (IIR) distribution in healthy controls (green), paroxysmal AF (lilac), and persistent AF (red) patients. The dashed line indicates the fibrosis threshold (IIR = 1.34), defined as the mean plus two standard deviations (SD) of the healthy control group's IIR values.

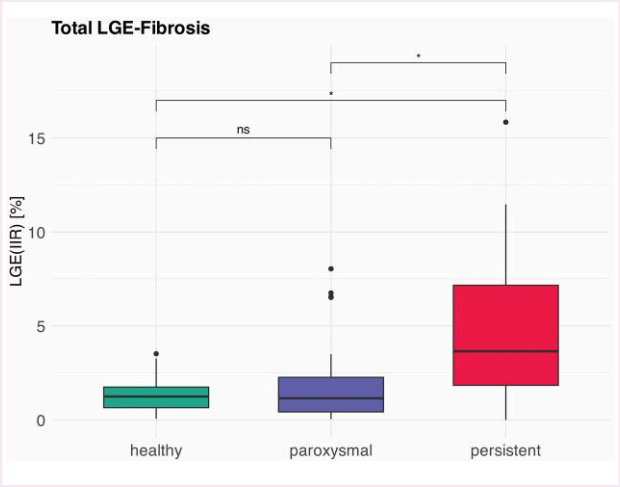

Figure 3 Total fibrosis burden, expressed as the number of surface cells with an IIR > 1.34, in healthy controls (green), paroxysmal AF (lilac), and persistent AF (red) patients. Statistical significance was assessed using Dunn's test with Bonferroni correction; bars and asterisks indicate significant differences (*P < 0.05; ns = not significant).

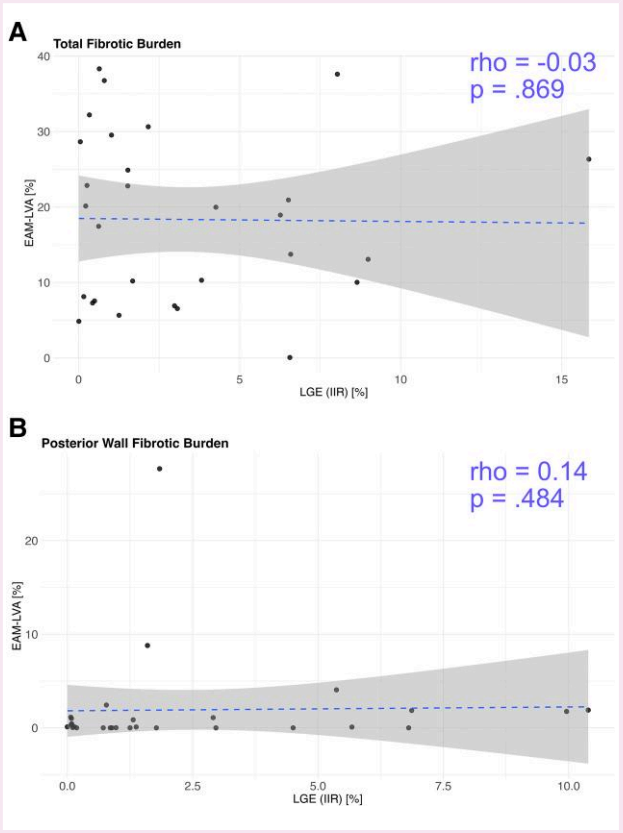

Figure 4 Correlation between total fibrosis burden on late gadolinium enhancement (LGE)—expressed as the percentage of surface cells with an image intensity ratio (IIR) > 1.34—and the percentage of low-voltage areas (LVA defined as regions with voltage < 0.5 mV) on bipolar electroanatomical mapping (EAM). No significant correlation was observed on a per-patient basis for the total left atrial surface (A) or the posterior wall (B).

baseline to follow-up in this area, whereas no significant change was observed in the remote LA myocardium 0.4% [−0.83–3.44], P = 0.169, see *Figure 7*.

Follow-up recurrence

Five patients experienced atrial arrhythmia recurrence. The median baseline LGE burden was numerically higher in these patients compared with those remaining in sinus rhythm (3.82% vs. 1.68%).

Intra-reader results

Ten randomly selected participants were analysed twice by the same reader more than three months apart. The ICC for LA-LGE was 0.99 (95%-confidence interval 0.95–0.99) with no significant bias (mean difference: 0.27%, P = 0.26). Bland-Altman plots are provided in the supplement.

Discussion

In this study, we used a high-resolution isotropic 3D LGE sequence to establish a setup-specific normality threshold for LA fibrosis based on a large healthy control group and validated the approach against EAM and follow-up imaging. An upper IIR normality threshold of 1.34 was identified. Applying this threshold, we found an increase in LA-LGE from paroxysmal to persistent AF. The method reliably detected ablation-induced scar, while no significant changes were observed in remote atrial regions after six months. However, no significant correlation was found between LA-LGE and EAM bipolar voltage at the patient and regional level, and only a weak point-by-point correlation was observed.

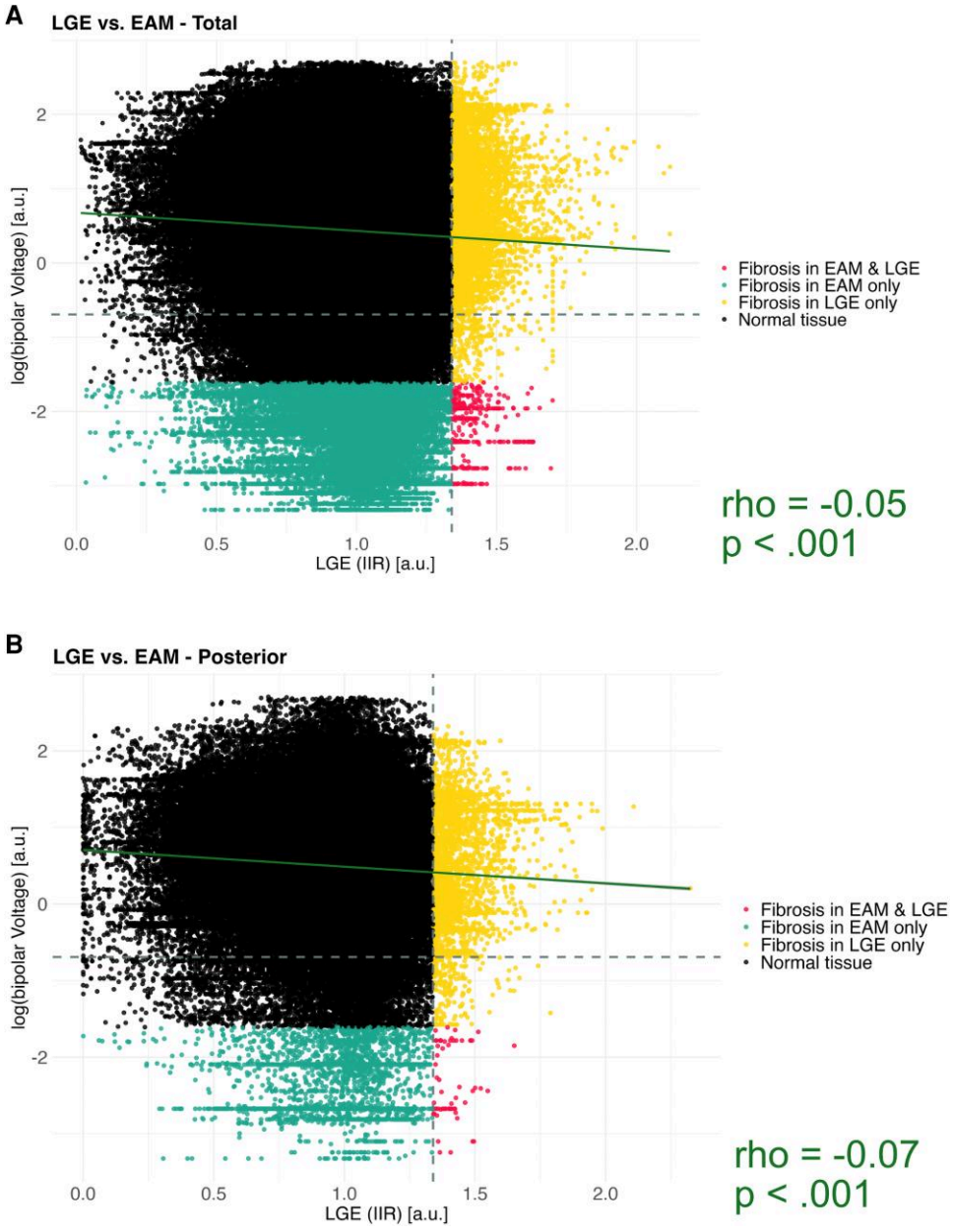

Figure 5 Point-by-point comparison of late gadolinium enhancement (LGE) and bipolar electroanatomical mapping (EAM) data after rigid and non-rigid registration for (*A*) the total left atrial (LA) surface and (*B*) the posterior LA wall. Only points within a maximum distance of 5 mm were included in the analysis. Colour code: black = healthy tissue (IIR < 1.34, voltage > 0.5 mV); yellow = fibrosis by LGE only (IIR > 1.34, voltage > 0.5 mV); turquoise = fibrosis by EAM only (IIR < 1.34, voltage < 0.5 mV); red = fibrosis by both modalities (IIR > 1.34, voltage < 0.5 mV). The y-axis is log-scaled for visualization purposes.

Technical considerations and fibrosis burden

Non-invasive assessment of LA fibrosis remains of clinical and research interest for personalized risk-stratification and prediction of ablation outcome.[9,25,26] Since early reports of LA-LGE, concerns have persisted that conventional sequences lack sufficient resolution to adequately depict the thin atrial wall.[27,28] Nevertheless, LGE, the gold standard for ventricular fibrosis imaging, remains promising for LA fibrosis assessment, provided further technical refinements. Compared with conventional anisotropic 3D LA-acquisitions, the sequence used here offers higher and isotropic spatial resolution (1.3 mm^3), reduces partial volume effects and avoids respiratory navigator artefacts.

Since LGE signal intensity is expressed on an arbitrary scale which varies between scans and centres, centre-specific thresholds are essential to avoid over- or underestimation of fibrosis.[21,29] Using a large healthy cohort, we derived an IIR threshold of 1.34, with fibrosis extent in controls consistent

with prior reports.[21,30] The observed increase in fibrosis from paroxysmal to persistent AF is consistent with histological and LGE studies,[2,4,21] although overall fibrosis extent in our cohort was low (persistent AF: median 3.65% [1.84–7.16]). In contrast, the DECAAF study reported a fibrosis burden ≥ 20% in 40% of patients.[9] However, Takahashi et al. reported a mean LA fibrosis fraction of 7.0 ± 3.8% in biopsy specimens from 230 AF patients (37% paroxysmal, 63% persistent or longstanding persistent AF).[4] Importantly, their study, consistent with other autopsy and biopsy data,[2,31] confirms that LA fibrosis in AF is a diffuse interstitial process. While LGE is the non-invasive gold standard for detecting focal replacement fibrosis in the left ventricle, its ability to visualize diffuse interstitial disease remains limited[32] and histological validation of LA-LGE is still scarce.[33] In addition, there was substantial overlap in IIR distributions between healthy controls and AF subgroups. Autopsy studies suggest that the overall burden of diffuse atrial fibrosis is relatively lower in the earlier stages of AF,[2] meaning that the majority of the atrial wall is still composed of relatively healthy myocardium. The substantial overlap in IIR distributions between groups may therefore largely reflect overlap in the signal characteristics of predominantly non-fibrotic atrial tissue.

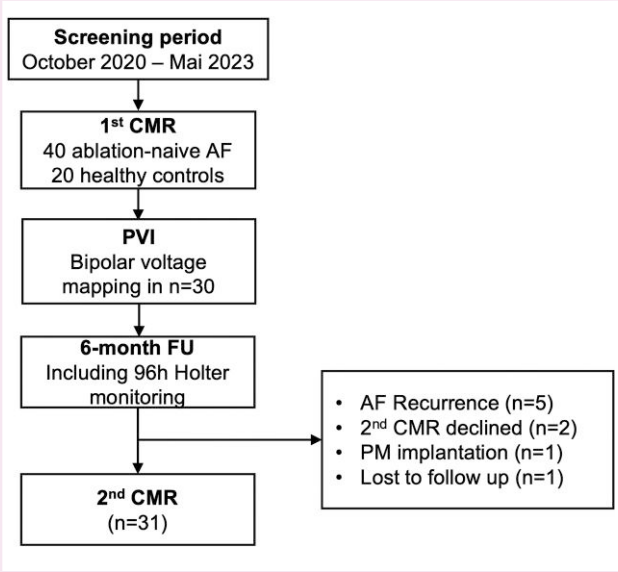

Figure 6 Study flow chart; AF, atrial fibrillation; CMR, cardiovascular magnetic resonance; PM, pacemaker; PVI, pulmonary vein isolation.

Correlation between LGE and EAM

Only a very weak correlation was observed between LA-LGE IIR and bipolar voltage from EAM, which is consistent with several reports,[13–15,34,35] although some studies have also shown stronger associations.[12,21,30,36] These discrepancies likely reflect differences in patient selection and methodology. Voltage amplitude is influenced by several factors such as wall thickness, heart rhythm, electrode size, and contact force,[28] whereas LGE measurements depend on acquisition parameters, contrast type, -dose, and -timing as well as post-processing techniques. In addition, correlations appear stronger in patients with advanced disease or prior ablation, where focal replacement fibrosis predominates.[29,37] In contrast, ablation-naïve patients, such as those in our study, typically exhibit diffuse interstitial fibrosis

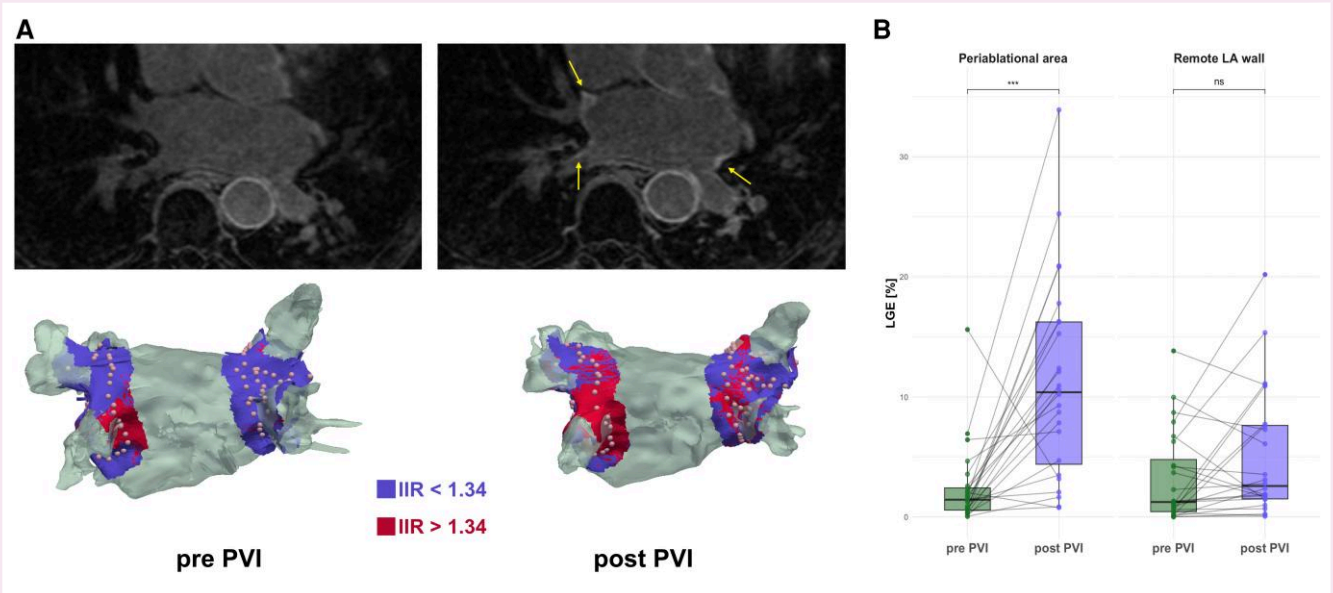

Figure 7 (*A*) Late gadolinium enhancement (LGE) images of the left atrium before (at baseline) and six months after pulmonary vein isolation (PVI). Yellow arrows indicate dense ablation induced scarring at follow-up. The corresponding 3D models show LGE quantification in the peri-ablational area (±7.5 mm from ablation sites) in comparison with the remote atrial wall (turquoise). Pulmonary veins and the mitral valve were excluded from remote myocardium analysis. Areas with IIR > 1.34 (scar) appear red; IIR < 1.34 (healthy myocardium) appear lilac. (*B*) Boxplots of total LGE extent before and after PVI demonstrate significant fibrosis increase in peri-ablational regions, with no significant change in remote myocardium. Significance was tested by paired Wilcoxon test (*$P < 0.05$; **$P < 0.01$; ***$P < 0.001$).

that is harder to visualize with LGE.[32] Biopsy studies support this interpretation: Takahashi et al. demonstrated diffuse interstitial fibrosis in all samples, with bipolar voltage correlating with fibrosis percentage.[4] Similarly, Yamaguchi et al. found that low-voltage areas are surrogates of diffuse remodelling rather than focal fibrosis.[31] Animal models of early atrial fibrosis have further shown that neither LGE nor EAM reliably capture early diffuse disease.[38] Emerging high-resolution T1 mapping may improve detection of diffuse LA fibrosis in the future.

Detection of ablation-induced scar

Ablation-related scar was consistently detected by LGE, with reproducible increases at ablation sites and no changes in remote LA regions. These results align with previous reports demonstrating excellent agreement between LGE, EAM and histology in detecting ablation induced scarring.[34,39] The difference in LGE visualization for ablation-related vs. AF-related fibrosis is pathophysiological: ablation lesions consist of dense, focal, transmural replacement fibrosis that is readily identified by LGE, whereas AF-related fibrosis is diffuse and interstitial, making it more difficult to visualize.[4,38] The lack of benefit from LGE-guided ablation strategies, as seen in DECAAF II,[7] likely reflects these limitations. Overall, our findings suggest that LA-LGE is more sensitive for detecting advanced remodelling and ablation-induced scarring than for early, diffuse, interstitial fibrosis in ablation-naïve AF patients.

Limitations

While both LGE and bipolar voltage have been validated against histology for detection of ablation scar, only EAM has been histologically validated for native diffuse LA fibrosis.[4] The density of EAM points was lower than in some more recent studies.[14] However, at the time the study was initiated, the number of mapping points acquired was comparable to that reported in many contemporary studies.[29]

The study population was relatively small, particularly for follow-up and recurrence analyses, and EAM was not available in all patients. Consequently, we were unable to perform adjustment for potential confounding factors, and the findings should therefore be interpreted as exploratory. Larger patient cohorts with longer follow-up are required to confirm prognostic implications of our findings, especially in relation to treatment outcomes.

Conclusions

High-resolution isotropic 3D LA-LGE allows robust detection of ablation-related scar and demonstrates biologically consistent associations between baseline fibrosis in ablation-naïve patients and AF persistence. However, its correlation with atrial bipolar voltage remains limited. These findings underscore the complementary roles of EAM and LGE and highlight the need for continued technical refinement, potentially including advanced T1 mapping, for comprehensive characterization of atrial fibrosis.

Supplementary data

Supplementary data are available at *European Heart Journal - Imaging Methods and Practice* online.

Author contributions

Maximilian Fenski (Conceptualization, Investigation, Methodology, Project administration, Supervision, Validation, Visualization, Writing—original draft, Writing—review & editing [lead], Data curation, Formal analysis [equal]), Richard Hickstein (Data curation, Formal analysis, Investigation, Methodology [equal], Software, Visualization, Writing—original draft, Writing—review & editing [lead]), Leo Krüger (Formal analysis, Investigation, Visualization [equal]), Clemens Ammann (Data curation, Software [equal]), Thomas Hadler (Data curation, Software [equal]), Karl Kunze (Resources [supporting]), Michaela Schmidt (Resources [supporting]), René M. Botnar (Resources, Software [equal]), Claudia Prieto (Resources, Software [equal]), André Rudolph (Conceptualization, Investigation, Methodology [equal]), Marcel Prothmann (Conceptualization, Investigation, Methodology [equal]), Michael Wiedemann (Conceptualization, Investigation, Methodology [equal]), Thomas H Grandy (Conceptualization, Investigation, Methodology [equal]), and Jeanette Schulz-Menger (Conceptualization, Funding acquisition, Resources, Supervision [lead], Writing—original draft, Writing—review & editing [equal])

Funding

Maximilian Fenski and Leo Dyke Krüger received funding from the German Heart Foundation. J.S.M. holds institutional grants from Charité—Universitätsmedizin Berlin, Germany. The funding sources had no role in the design of the study, data collection, analysis, interpretation, or manuscript preparation.

Conflict of interest: Karl Kunze is an employee of Siemens Healthcare Limited, UK. Michaela Schmidt is an employee of Siemens Healthineers AG, Germany. These relationships did not interfere with or influence the conduct of the research or the interpretation of the data. All other authors declare that they have no relationships relevant to the content of this publication to disclose.

Data availability

The data underlying this study are not publicly available due to restrictions imposed by local data protection regulations. Selected anonymized data may be made available upon reasonable request to the corresponding author.

Lead Author Biography

Maximilian Fenski, MD is a board-certified specialist in internal medicine and currently in advanced training in cardiology. His clinical and research interests focus on cardiovascular magnetic resonance imaging and cardiac electrophysiology. He completed a two-year research fellowship at the University of Oxford, where his work focused on the impact of weight loss in patients with heart failure with reduced ejection fraction (HFrEF) and obesity. Since 2018, he has been an active researcher in the Cardiac MRI group at Charité – Universitätsmedizin Berlin, with a particular focus on the validation of techniques for the assessment of left atrial myopathy.

References

1. Shen MJ, Arora R, Jalife J. Atrial myopathy. *JACC Basic Transl Sci* 2019;**4**:640–54.
2. Platonov PG, Mitrofanova LB, Orshanskaya V, Ho SY. Structural abnormalities in atrial walls are associated with presence and persistency of atrial fibrillation but not with age. *J Am Coll Cardiol* 2011;**58**:2225–32.

3. King JB, Azadani PN, Suksaranjit P, Bress AP, Witt DM, Han FT *et al.* Left atrial fibrosis and risk of cerebrovascular and cardiovascular events in patients with atrial fibrillation. *J Am Coll Cardiol* 2017;**70**:1311–21.
4. Takahashi Y, Yamaguchi T, Otsubo T, Nakashima K, Shinzato K, Osako R *et al.* Histological validation of atrial structural remodelling in patients with atrial fibrillation. *Eur Heart J* 2023;**44**:3339–53.
5. Rolf S, Kircher S, Arya A, Eitel C, Sommer P, Richter S *et al.* Tailored atrial substrate modification based on low-voltage areas in catheter ablation of atrial fibrillation. *Circ Arrhythm Electrophysiol* 2014;**7**:825–33.
6. Quail M, Grunseich K, Baldassarre LA, Mojibian H, Marieb MA, Cornfeld D *et al.* Prognostic and functional implications of left atrial late gadolinium enhancement cardiovascular magnetic resonance. *J Cardiovasc Magn Reson* 2019;**21**:2.
7. Marrouche NF, Wazni O, McGann C, Greene T, Dean JM, Dagher L *et al.* Effect of MRI-guided fibrosis ablation vs conventional catheter ablation on atrial arrhythmia recurrence in patients with persistent atrial fibrillation: the DECAAF II randomized clinical trial. *JAMA* 2022;**327**:2296–305.
8. Bisbal F, Guiu E, Cabanas-Grandío P, Berruezo A, Prat-Gonzalez S, Vidal B *et al.* CMR-guided approach to localize and ablate gaps in repeat AF ablation procedure. *JACC Cardiovasc Imaging* 2014;**7**:653–63.
9. Marrouche NF, Wilber D, Hindricks G, Jais P, Akoum N, Marchlinski F *et al.* Association of atrial tissue fibrosis identified by delayed enhancement MRI and atrial fibrillation catheter ablation: the DECAAF study. *JAMA* 2014;**311**:498–506.
10. Regany-Closa M, Pomes-Perez J, Invers-Rubio E, Borras R, Pellicer-Sendra B, Prat-Gonzalez S *et al.* Head-to-head comparison of pulsed-field ablation, high-power short-duration ablation, cryoballoon and conventional radiofrequency ablation by MRI-based ablation lesion assessment. *J Interv Card Electrophysiol* 2025. https://doi.org/10.1007/s10840-025-02086-9.
11. Khurram IM, Beinart R, Zipunnikov V, Dewire J, Yarmohammadi H, Sasaki T *et al.* Magnetic resonance image intensity ratio, a normalized measure to enable interpatient comparability of left atrial fibrosis. *Heart Rhythm* 2014;**11**:85–92.
12. Zghaib T, Keramati A, Chrispin J, Huang D, Balouch MA, Ciuffo L *et al.* Multimodal examination of atrial fibrillation substrate: correlation of left atrial bipolar voltage using multi-electrode fast automated mapping, point-by-point mapping, and magnetic resonance image intensity ratio. *JACC Clin Electrophysiol* 2018;**4**:59–68.
13. Sramko M, Peichl P, Wichterle D, Tintera J, Weichet J, Maxian R *et al.* Clinical value of assessment of left atrial late gadolinium enhancement in patients undergoing ablation of atrial fibrillation. *Int J Cardiol* 2015;**179**:351–7.
14. Eichenlaub M, Mueller-Edenborn B, Minners J, Figueras I, Ventura RM, Forcada BR *et al.* Comparison of various late gadolinium enhancement magnetic resonance imaging methods with high-definition voltage and activation mapping for detection of atrial cardiomyopathy. *Europace* 2022;**24**:1102–11.
15. Chen J, Arentz T, Cochet H, Müller-Edenborn B, Kim S, Moreno-Weidmann Z *et al.* Extent and spatial distribution of left atrial arrhythmogenic sites, late gadolinium enhancement at magnetic resonance imaging, and low-voltage areas in patients with persistent atrial fibrillation: comparison of imaging vs. Electrical parameters of fibrosis and arrhythmogenesis. *Europace* 2019;**21**:1484–93.
16. Platonov PG, Ivanov V, Ho SY, Mitrofanova L. Left atrial posterior wall thickness in patients with and without atrial fibrillation: data from 298 consecutive autopsies. *J Cardiovasc Electrophysiol* 2008;**19**:689–92.
17. Mulder MJ, Keuken MC, Bazin PL, Alkemade A, Forstmann BU. Size and shape matter: the impact of voxel geometry on the identification of small nuclei. *PLoS One* 2019;**14**:e0215382.
18. Munoz C, Bustin A, Neji R, Kunze KP, Forman C, Schmidt M *et al.* Motion-corrected 3D whole-heart water-fat high-resolution late gadolinium enhancement cardiovascular magnetic resonance imaging. *J Cardiovasc Magn Reson* 2020;**22**:53.
19. Hindricks G, Potpara T, Dagres N, Arbelo E, Bax JJ, Blomström-Lundqvist C *et al.* 2020 ESC Guidelines for the diagnosis and management of atrial fibrillation developed in collaboration with the European Association for Cardio-Thoracic Surgery (EACTS). *Eur Heart J* 2021;**42**:373–498.
20. Razeghi O, Solís-Lemus JA, Lee AWC, Karim R, Corrado C, Roney CH *et al.* CemrgApp: an interactive medical imaging application with image processing, computer vision, and machine learning toolkits for cardiovascular research. *SoftwareX* 2020;**12**:100570.
21. Benito EM, Carlosena-Remirez A, Guasch E, Prat-González S, Perea RJ, Figueras R *et al.* Left atrial fibrosis quantification by late gadolinium-enhanced magnetic resonance: a new method to standardize the thresholds for reproducibility. *Europace* 2017;**19**:1272–9.
22. Schulz-Menger J, Bluemke DA, Bremerich J, Flamm SD, Fogel MA, Friedrich MG *et al.* Standardized image interpretation and post-processing in cardiovascular magnetic resonance—2020 update: Society for Cardiovascular Magnetic Resonance (SCMR): board of trustees task force on standardized post-processing. *J Cardiovasc Magn Reson* 2020;**22**:19.
23. Althoff TF, Anderson RH, Goetz C, Petersen SE, Díaz PM, Nijveldt R *et al.* Regionalization of the atria for 3D electroanatomical mapping, cardiac imaging, and computational modelling: a clinical consensus statement of the European Heart Rhythm Association and the European Association of Cardiovascular Imaging of the ESC. *Europace* 2025;**27**:euaf134.
24. Deneke T, Khargi K, Müller KM, Lemke B, Mügge A, Laczkovics A *et al.* Histopathology of intraoperatively induced linear radiofrequency ablation lesions in patients with chronic atrial fibrillation. *Eur Heart J* 2005;**26**:1797–803.
25. Huo Y, Gaspar T, Schönbauer R, Wójcik M, Fiedler L, Roithinger FX *et al.* Low-voltage myocardium-guided ablation trial of persistent atrial fibrillation. *NEJM Evid* 2022;**1**:EVIDoa2200141.
26. Verma A, Wazni OM, Marrouche NF, Martin DO, Kilicaslan F, Minor S *et al.* Pre-existent left atrial scarring in patients undergoing pulmonary vein antrum isolation: an independent predictor of procedural failure. *J Am Coll Cardiol* 2005;**45**:285–92.
27. Appelbaum E, Manning WJ. Left atrial fibrosis by late gadolinium enhancement cardiovascular magnetic resonance predicts recurrence of atrial fibrillation after pulmonary vein isolation: do you see what I see? *Circ Arrhythm Electrophysiol* 2014;**7**:2–4.
28. Tzeis S, Gerstenfeld EP, Kalman J, Saad EB, Sepehri Shamloo A, Andrade JG *et al.* 2024 European Heart Rhythm Association/Heart Rhythm Society/Asia Pacific Heart Rhythm Society/Latin American Heart Rhythm Society expert consensus statement on catheter and surgical ablation of atrial fibrillation. *Europace* 2024;**26**:euae043.
29. Bijvoet GP, Nies HMJM, Holtackers RJ, Linz D, Adriaans BP, Nijveldt R *et al.* Correlation between cardiac MRI and voltage mapping in evaluating atrial fibrosis: a systematic review. *Radiol Cardiothorac Imaging* 2022;**4**:e220061.
30. Oakes RS, Badger TJ, Kholmovski EG, Akoum N, Burgon NS, Fish EN *et al.* Detection and quantification of left atrial structural remodeling with delayed-enhancement magnetic resonance imaging in patients with atrial fibrillation. *Circulation* 2009;**119**:1758–67.
31. Yamaguchi T, Otsubo T, Takahashi Y, Nakashima K, Fukui A, Hirota K *et al.* Atrial structural remodeling in patients with atrial fibrillation is a diffuse fibrotic process: evidence from high-density voltage mapping and atrial biopsy. *J Am Heart Assoc* 2022;**11**:e024521.
32. Sibley CT, Noureldin RA, Gai N, Nacif MS, Liu S, Turkbey EB *et al.* T1 mapping in cardiomyopathy at cardiac MR: comparison with endomyocardial biopsy. *Radiology* 2012;**265**:724–32.
33. McGann C, Akoum N, Patel A, Kholmovski E, Revelo P, Damal K *et al.* Atrial fibrillation ablation outcome is predicted by left atrial remodeling on MRI. *Circ Arrhythm Electrophysiol* 2014;**7**:23–30.
34. Harrison JL, Jensen HK, Peel SA, Chiribiri A, Grondal AK, Bloch LO *et al.* Cardiac magnetic resonance and electroanatomical mapping of acute and chronic atrial ablation injury: a histological validation study. *Eur Heart J* 2014;**35**:1486–95.
35. Nairn D, Eichenlaub M, Lehrmann H, Müller-Edenborn B, Chen J, Huang T *et al.* Spatial correlation of left atrial low voltage substrate in sinus rhythm versus atrial fibrillation: the rhythm specificity of atrial low voltage substrate. *J Cardiovasc Electrophysiol* 2023;**34**:1613–21.
36. Caixal G, Alarcón F, Althoff TF, Nuñez-Garcia M, Benito EM, Borràs R *et al.* Accuracy of left atrial fibrosis detection with cardiac magnetic resonance: correlation of late gadolinium enhancement with endocardial voltage and conduction velocity. *Europace* 2021;**23**:380–8.
37. Kuo L, Zado E, Frankel D, Santangeli P, Arkles J, Han Y *et al.* Association of left atrial high-resolution late gadolinium enhancement on cardiac magnetic resonance with electrogram abnormalities beyond voltage in patients with atrial fibrillation. *Circ Arrhythm Electrophysiol* 2020;**13**:e007586.
38. Wilk B, Lim H, Hicks J, Sullivan R, Thiessen JD, Kovacs M *et al.* Complexities of atrial fibrosis imaging: exploring relationships between endocardial voltage, extracellular volume, and sympathetic innervation. *JACC Clin Electrophysiol* 2025;**11**:735–48.
39. Chubb H, Karim R, Roujol S, Nuñez-Garcia M, Williams SE, Whitaker J *et al.* The reproducibility of late gadolinium enhancement cardiovascular magnetic resonance imaging of post-ablation atrial scar: a cross-over study. *J Cardiovasc Magn Reson* 2018;**20**:21.